Physicochem. Probl. Miner. Process., 61(6), 2025, 216095

http://www.journalssystem.com/ppmp

Physicochemical Problems of Mineral Processing

ISSN 1643-1049

PHB/chitosan microspheres as green collectors for quartz flotation

Klaudia W. Zaręba [1], Dominik Kosior [1], Przemyslaw B. Kowalczuk [2], Anna Faruga [1], Maciej Guzik [1], Jan Zawala [1]

[1] Jerzy Haber Institute of Catalysis and Surface Chemistry, Polish Academy of Sciences, Niezapominajek 8, PL-30239 Krakow, Poland

[2] Norwegian University of Science and Technology, Department of Geosciences, S. P. Andersens veg 15a, 7031 Trondheim, Norway

Corresponding author: klaudia.zareba@ikifp.edu.pl, jan.zawala@ikifp.edu.pl

Abstract: This study investigates biopolymer poly(3-hydroxybutyrate) microspheres coated with chitosan as a potential biodegradable and environmentally friendly collector for froth quartz flotation. The work includes physicochemical characterization of PHB/CHI particles including their zeta potential (+52,36 mV at pH 4,58), assessment of their hydrophobic behavior in water and in the presence of nonionic frother 4-methyl-2-pentanol (MIBC) through contact angle measurement and three-phase contact (TPC) formation time. The results show that adsorption PHB/CHI microspheres onto glass plate increases surface hydrophobicity, yielding a maximum contact angle of $\approx$ 50°, accelerates TPC formation, significantly enhances flotation recovery, with clear dosage dependent improvements in flotation kinetics. Even low collector dosage (0.08 mg per 1 g of quartz) yielded high quartz recoveries of around 80%. Experiments using the particle–bubble dynamic attachment apparatus further confirmed the enhanced hydrophobization mechanism, revealing substantially higher bubble coverage in the presence of PHB/CHI. In contrast, chitosan alone resulted in negligible attachment, and the addition of MIBC did not significantly influence bubble coverage. Overall, these preliminary findings demonstrate the novelty and promise of PHB/CHI microspheres as an effective green alternative to conventional amine collectors, with their polydispersity and potential to bind fine particles further contributing to improved flotation efficiency.

***Keywords*:** flotation, poly(3-hydroxybutyrate), PHB particles, chitosan

1. Introduction

Flotation is a widely applied physicochemical separation technique that utilizes the attachment of gas bubbles to selectively separate hydrophobic particles from aqueous suspensions. Developed initially for mineral beneficiation, flotation has broadened its applications to areas such as wastewater treatment and environmental remediation (Jiang et al., 2022; Peleka et al., 2018; Rubio et al., 2002).

Quartz is one of the most common gangue minerals present in metal ores. Its removal is often achieved by reverse flotation, which selectively renders quartz hydrophobic through collector adsorption (Araujo et al., 2005; Gungoren et al., 2025; Han et al., 2018; Wiertel-Pochopien and Zawala, 2019; Zawala et al., 2017). High separation efficiency can be achieved through the application of both cationic and anionic reverse flotation methods (Han et al., 2018; Kordloo et al., 2023; Lima et al., 2013). The mechanism of reverse flotation relies on the selective adsorption of collectors on the surface of gangue minerals, which enhances their hydrophobicity and enables efficient separation from the valuable mineral phase (Zawala et al., 2017). Flotation relies on various chemicals, such as collectors and frothers, to control the surface properties of particles and bubbles. Collectors render selected mineral surfaces hydrophobic, enabling their attachment to air bubbles (Abarca et al., 2018; Laskowski, 2010), while frothers form and stabilize the froth by reducing bubble coalescence (Melo and Laskowski, 2006; Pawliszak et al., 2024a, 2024b). Additionally, modifiers such as activators, depressants, and pH

DOI: 10.37190/ppmp/216095

regulators are used to enhance selectivity and improve separation efficiency (Herrera Urbina, 2003; Nagaraj and Farinato, 2016)

Most flotation reagents are petrochemical-based compounds that degrade slowly in the environment, leading to water pollution, eutrophication, and bioaccumulation in living organisms. In froth flotation, collectors are key reagents responsible for selectively adsorbing onto mineral surface and imparting hydrophobicity, enabling their attachment to air bubbles. Their complexity is steadily increasing, as reflected by the development of nanoparticle-based collectors (Abarca et al., 2015; Hajati et al., 2016; Nasirimoghaddam et al., 2020; Yang et al., 2011). One promising direction involves bio-collectors, a class of bio-based flotation reagent derived from natural and biodegradable compounds. These bio-collectors have similar function to traditional collectors, but their renewable origin and improved environmental compatibility make them an attractive replacement for conventional petrochemical formulations (Asimi Neisiani et al., 2023; Budemberg et al., 2025; Dhar et al., 2021; Legawiec et al., 2023a; Tohry et al., 2021). For this reason, some researchers have focused on bio-polymers produced by bacterial fermentation, which represent more advanced and environmentally friendly alternatives to traditional flotation reagents (Bednarek et al., 2025; Ramos-Escobedo et al., 2016; Sigauke et al., 2025; Yang et al., 2014).

In this context, polyhydroxyalkanoates appear to be an attractive alternative to conventional flotation chemicals (Behera and Mulaba-Bafubiandi, 2017; Govender and Gericke, 2011; Rehm, 2010). Polyhydroxyalkanoates (PHAs) are a family of biopolymers synthesized by many bacteria during the fermentation of sugars and lipids as storage materials. Among them, poly(3-hydroxybutyrate) (PHB) deserves special attention due to its favorable mechanical properties and thermoplasticity, which are comparable to those of petroleum-derived polymers such as polypropylene and polyethylene (Ganapathy et al., 2018; McAdam et al., 2020; Rajan et al., 2019). Its properties can be further tailored through blending with other polymers, synthesizing copolymers, or incorporating functional groups and plasticizers (McAdam et al., 2020; Zhang and Thomas, 2011). Importantly, PHB undergoes microbial degradation to CO_2 and H_2O, which microorganisms can readily assimilate, and this process might be further accelerated by UV irradiation (Altaee et al., 2016). Poly(3-hydroxybutyrate) (PHB) microspheres can be produced using a solid–in–oil–water (s/o/w) emulsion solvent evaporation method, which allows control of particle size through parameters such as polymer concentration, surfactant content, and stirring rate (Francis et al., 2010; Wei et al., 2018; Zalloum et al., 2019). For example, faster mixing and higher poly(vinyl alcohol) (PVA) concentrations yield smaller particles, while higher polymer molar mass narrows the size distribution (Francis et al., 2011; Wei et al., 2018)

Although PVA is an effective stabilizer, its persistence and slow biodegradation in aquatic systems raise environmental concerns (Francis et al., 2011; Marušincová et al., 2013; Olalla et al., 2021; Ye et al., 2017). Chitosan has therefore emerged as a sustainable alternative to PVA in flotation systems, as it is biodegradable, biocompatible, and can be chemically modified to tailor its surface activity and selectivity toward specific minerals (Chiellini et al., 2003; Leceta et al., 2013; Peter, 1995; Sawaguchi et al., 2015). Chitosan, a natural cationic polysaccharide rich in amino and hydroxyl functional groups, exhibits strong hydrophilic character and can act as an effective depressant in flotation processes (Cohen and Poverenov, 2022; Zargar et al., 2015). Through its adsorption onto specific mineral surfaces via chemisorption involving amine and hydroxyl groups, chitosan increases hydrophilicity, inhibiting bubble-mineral attachment and suppressing undesired flotation of the depressed phase (Tiraferri et al., 2014). It has been successfully used to selectively depress chalocopryrite, pyrite and galena, enabling enhanced separation from target minerals (Alsafasfeh et al., 2023; Hayat et al., 2017; Zhang et al., 2019). Recent studies have further expanded its applicability, for example chitosan (10 kDa) enabled efficient reverse flotation of pyrite from galena via stronger adsorption and increased surface hydrophilicity (Zhang et al., 2019). These studies confirm potential chitosan as an eco-friendly depressant in mineral flotation. Moreover, due to its strong affinity for mineral surfaces rich in hydroxyl groups, chitosan and its derivatives are promising reagents for reverse flotation of quartz, where selective depression of other minerals combined and simultaneous hydrophobization of silica can offer an environmentally friendly alternative to conventional collectors.

In this study, we investigated poly(3-hydroxybutyrate) (PHB) microspheres coated with chitosan as potential biodegradable collectors for flotation of quartz. The main objective was to characterize their

surface properties, including particle size, charge, wettability and to examine their interaction with negatively charged glass surfaces. The hydrophobicity of the PHB microspheres was assessed trough contact angle measurements, while the three – phase contact time was determined to evaluate bubble – particle attachment dynamics. Finally, laboratory flotation tests of quartz were conducted to assess the performance of PHB microspheres as a green alternative to conventional collectors.

2. Materials and methods

2.1. Materials

Methyl isobutyl carbinol (MIBC) (Sigma-Aldrich, ⩾98%) was used as a frother. Chitosan (Sigma-Aldrich, ⩾98%, molecular weight 50,000 – 190,000 Da), acetic acid (Chempur, ⩾99,5%), and chloroform (Chempur, ⩾99,5%) were commercially available reagents used in the preparation of microspheres. The ionic strength and the pH were adjusted with respective solutions of analytical grade NaCl (SigmaAldrich, ⩾99,5%), NaOH (Chempur, ⩾98%), and HCl (Chempur, 35-38%). Ultrapure Milli-Q water (Merck Millipore, resistivity of 18 MΩ·cm at 25°C) was used for preparation of solutions. Ethyl alcohol (Chempur, ⩾96%), H_2SO_4 (Chempur, ⩾95%) and H_2O_2 (Chempur, 30%) were used to purify a borosilicate glass.

Borosilicate glass plates were used for contact angle, three-phase contact formation experiments and SEM imaging, while high-purity natural quartz samples for flotation tests and particle-bubble dynamic attachment apparatus.

Borosilicate glass plates were purified before each measurement according to the following procedure: (i) in the first stage, the borosilicate glass was immersed in ethyl alcohol and sonicated for 20 min and next thoroughly rinsed in distilled water; (ii) in the second stage, the glass plate was transferred to the piranha solution (a 1:1 mixture of H_2SO_4 and H_2O_2). The glass was immersed in this solution for 30 minutes. After cleaning in the piranha solution, the holder with the glass was removed again and the glass was rinsed several times in distilled water.

The high-purity natural quartz sample originated from a mine in Norway. The material was mechanically ground and wet-sieved to obtain the desired particle size fractions, and the 50–100 μm fraction was selected for flotation and particle-bubble attachment studies.

2.2. Preparation of poly(3-hydroxybutyrate) microspheres

Poly(3-hydroxybutyrate) (PHB) was produced and purified at the Bioprocess Development Laboratory, Jerzy Haber Institute of Catalysis and Surface Chemistry (Krakow, Poland). PHB was obtained using Zobellella denitrificans strain MW1 grown on glycerol as the sole carbon source (Faruga et al., 2025; Ibrahim and Steinbüchel, 2009).

Poly(3-hydroxybutyrate) (PHB) microspheres were prepared as follows: first, a chitosan solution was prepared by dissolving 1 g of chitosan in 100 mL of 0.015 mol/L NaCl solution, followed by the addition of 2.9 mL of 99.5% acetic acid. The mixture was stirred for 2 h at 75 °C in a covered vessel to minimalize water evaporation and then for 18 h at room temperature. Separately, a 1% PHB solution was prepared by dissolving 0.1 g of the polymer in 10 mL of chloroform. Next, 50 mL of the chitosan solution was taken, and the PHB solution was added dropwise through a 23G (outer diameter 0,64 mm) stainless steel needle. The resulting mixture was stirred on a magnetic stirrer (stir bar length: 2 cm; stirring speed: 2000 rpm) for 24 h. To remove excess chitosan, the suspension was centrifuged three times (4000 rpm, 8 min each), with washing in distilled water after each cycle. Because chloroform is highly volatile, it evaporated during the 24 h stirring period, and the subsequent centrifugation and washing steps ensured the removal of both residual chloroform and acetic acid from the final PHB/CHI microspheres. The pH solution was equal 3.56 during mixing and 4.58 after centrifugation. The product, i.e., poly(3-hydroxybutyrate) coated with chitosan, will be referred to as PHB/CHI microspheres.

2.3. Scanning electron microscopy

The surface morphology of the PHB/CHI microspheres was studied using a high-resolution scanning electron microscope (JEOL JSM-7500F) equipped with an AZtecLiveLite Xplore 30 attachment and a secondary electron detector. The microspheres were deposited on a glass plate by diffusion from the

solution for 30 minutes. Prior to imaging, all samples were coated with a 40 nm thick chromium layer using a K575X sputtering system.

2.4. Zeta potential

The zeta potential was determined by the Electronic Light Scattering (ELS) method, used Zetasizer Nano Series from Malvern Instruments. Each value was calculated as the average of three consecutive runs of the instrument, with a minimum of 20 measurement taken during each run.

2.5. Contact angle measurement

Advancing contact angle (Θ_A) measurements were performed using the sessile drop method on a Krüss DSA100 apparatus. Prior to measurement, the clean borosilicate glass plates were immersed in a 10 mg/L PHB/CHI solution for varying time periods to examine the influence of adsorption time on surface wettability. A droplet of constant volume (ca. 2 μL) was dispensed using a needle with a 0.5 mm outer diameter. A CCD camera coupled with a digital recording system and DSA4 software was used to capture and analyze the droplet profile.

2.6. Three phase contact formation measurement

Three-phase contact (TPC) formation of bubble on the surface of borosilicate glass plates coated with PHB/CHI was studied using a setup consisting of a borosilicate glass column (290 × 50 × 50 mm) with a capillary (inner diameter 0.075 mm) at the bottom, connected to a 'bubble-on-demand' apparatus (Zawala and Niecikowska, 2017). The equivalent diameter of the bubble (deq) detaching from the capillary was 1.48 ± 0.01 mm in Milli-Q water. Prior to measurement, the glass plate was thoroughly cleaned and subsequently immersed in a 10 mg/L PHB/CHI solution for various deposition time (tdep). Next, the coated solid plate was positioned horizontally beneath the solution surface at a distance L = 300 mm from the capillary orifice. Bubble collisions, bouncing, and attachment to solid surfaces were monitored using a high-speed camera (IDT NX5, 1000 fps).

In general, the time of three-phase contact formation (t_{TPC}) can be considered as the sum of the bubble bouncing time ($t_{bouncing}$) and the film drainage time ($t_{drainage}$) (Legawiec et al., 2023b):

$$t_{TPC} = t_{bouncing} + t_{drainage} \quad (1)$$

Both parameters tbouncing and $t_{drainage}$ are crucial for interpreting particle – bubble attachment dynamic. The $t_{bouncing}$ was calculated from high – speed image sequences as the period between first contact of the bubble with the solid surface and the last reflection before a stable liquid film was formed. In contrast, $t_{drainage}$ represent the subsequent step, during the liquid film separating the bubble and solid thins until rupture and attachment. The contributions of these two steps provide valuable information on the interactions of surface forces and wettability, describing bubble – solid attachment efficiency.

Once TPC was formed and TPC line stopped moving, the receding contact angle (Θ_R) (captive bubble method) was measured using a custom Python script with the PIL module (Wiertel-Pochopien et al., 2021).

Each experiment was repeated 10–20 times to get reliable data. Further details of the experimental set-up and determination of the bubble velocity have been described elsewhere (Kosior et al., 2014; Krasowska and Malysa, 2007; Malysa et al., 2005).

2.7. Particle-bubble dynamic attachment apparatus

Fig. 1 schematically presents the set-up used to study particle-bubble– attachment under dynamic conditions. The set-up consisted of a glass cell (50 × 50 × 50 mm) filled with 100 mL of the PHB/CHI microsphere solution and a magnetic stirrer placed at the bottom. Before each experiment, 5 g of quartz (particle size 50–100 μm) was added and conditioned for 4 min under continuous stirring, after which MIBC as a frother was introduced and stirred for an additional 4 min. These conditions were selected to maintain consistency with the flotation procedure, in which identical conditioning time, stirring, reagent addition sequence and quantities were applied. A stainless-steel needle with an outer diameter of 1.82 mm was then immersed 20 mm below the liquid surface. A bubble of 2.5 mm in diameter was

generated at the capillary tip using a peristaltic pump driven by a stepper motor, enabling precise control of the bubble volume. The camera (ArduCam IMX477 with an AF Micro Nikkor 60 mm lens) was positioned laterally to the cell for real-time monitoring. Once the bubble was formed, the slurry was stirred for an additional 1 min. After stirring was stopped and the quartz had settled, two photographs of the bubble–grains aggregate were taken: the first under white light (Fig. 2A), and the second with all lights off and the bubble illuminated by a red laser (Fig. 2B).

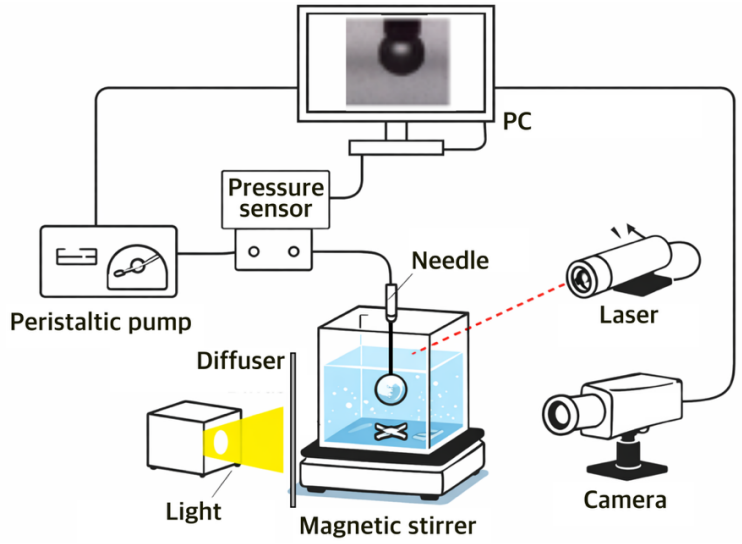

Fig 1. Schematic view of an experimental set-up

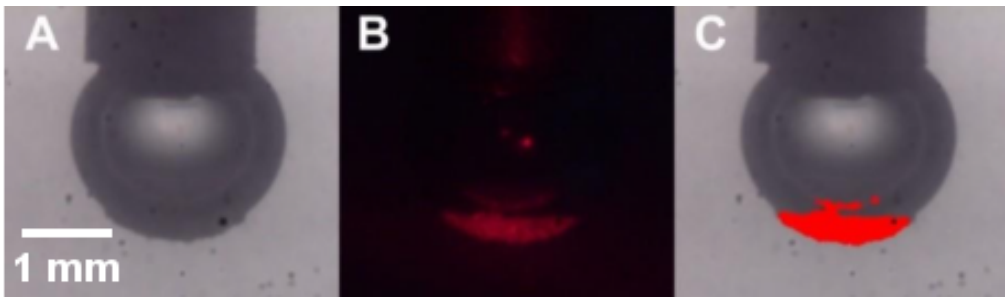

Fig. 2. Images of the particle-bubble attachment: (A) under white light illumination, (B) under red laser illumination, and (C) post-processed image

In post-processing, two photographs were merged to produce a final image, which was then analyzed using ImageJ software to determine the cross-sectional area of the entire bubble (A_{bubble}) and the area covered by quartz particles (A_{quartz}). Using this data the bubble surface coverage was calculated:

$$Coverage = \frac{A_{bubble}}{A_{quartz}} \cdot 100\% \quad (2)$$

The calculated bubble surface coverage reflects the degree of particle–bubble attachment observed under the given experimental conditions.

2.8. Particle Size Distribution

The quartz used in this study originated from the same Norwegian deposit as the material characterized in detail in (Larsen et al., 2019), where XRD analysis confirmed its high mineralogical purity. In the present work, the quartz was mechanically ground and wet-sieved using sieves with a mesh size of 50–100 µm. The grains were dried in a chamber at 90°C. The particle size distribution was measured using laser diffraction with a Malvern Metasizer 2000. Fig. 3 shows the particle size distribution of the quartz used in the experiments. The quartz sample used in the flotation experiments had a particle size distribution characterized by D10 = 28.0 µm, D50 = 58.9 µm, and D90 = 101 µm (Fig. 3).

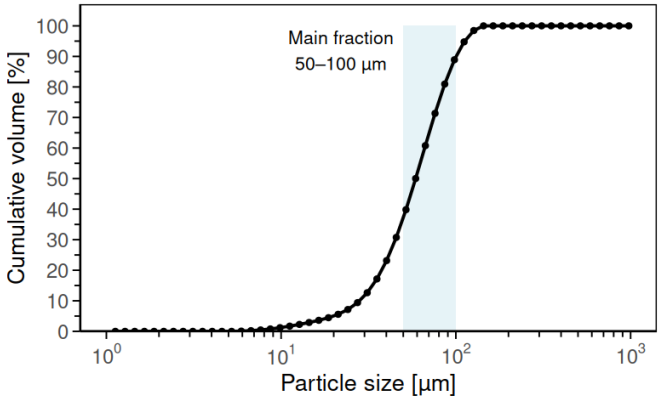

Fig. 3. Particle size distribution of quartz

2.9. Flotation

Flotation experiments were conducted in a 500 mL column using a laboratory Maelgwyn mechanical flotation machine. In each test, 25 g of quartz fraction (particle size 50–100 µm) was dispersed in the PHB/CHI microsphere solution of the desired concentration. The slurry was conditioned for 4 minutes, after which the frother MIBC 1.6×10^{-2} M was added and stirred for an additional 4 minutes at an impeller rotation speed of 1800 rpm. Following conditioning, the air flow 50 l/h was initiated, while impeller rotation speed kept constant (1800 rpm). The flotation parameters were determined experimentally. The impeller rotation speed was adjusted to the specific flotation machine used, while the MIBC concentration was selected based on the observed froth height and stability under the applied operating conditions. Once selected in preliminary tests, the MIBC dosage was kept constant in all flotation experiments, ensuring full adherence to the principle of controlling variables. The froth was collected in several weighed cuvettes, which were changed at specific time intervals after 1, 2, 3, 6 minutes and subsequently after 10 minutes, to account for the higher flotation rate at the beginning process. The cuvettes with flotation products were dried in an oven at 100° degrees, and then weighed to calculate the quartz recovery (in this case the product yield corresponds to the recovery).

All experiments in this study were carried out at room temperature, approximately 24 ±1°C. Depending on the type of experiment, measurements were performed between three and ten times to asses repeatability.

3. Results and discussion

3.1. Physicochemical properties of PHB/CHI microspheres in bulk

The physicochemical characteristic of PHB/CHI microspheres, determined from zeta potential and SEM analyses, indicates that the microspheres exhibit a well-defined spherical shape with distinctly rough surfaces, likely due to the morphology of the PHB matrix and the structure of the chitosan coating layer (Fig .4).

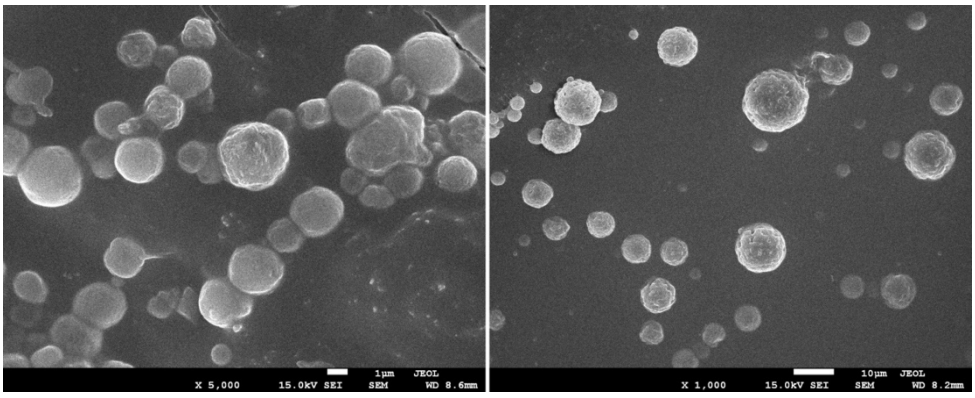

Fig. 4. SEM images of PHB/CHI microspheres

Furthermore, a qualitative analysis of the images indicates that the PHB/CHI microsphere suspension is highly polydisperse. Particle size distribution analysis (Fig. 5) confirmed that most microspheres ranged between 800 and 1200 nm, with a broad overall distribution extending up to about 3000 nm. Although a few larger particles (5–10 μm) are visible in the SEM images, they occur only sporadically in the sample (<1–2%) and therefore do not significantly affect the particle size distribution shown in Fig. 5, which represents the dominant population of PHB/CHI microspheres.

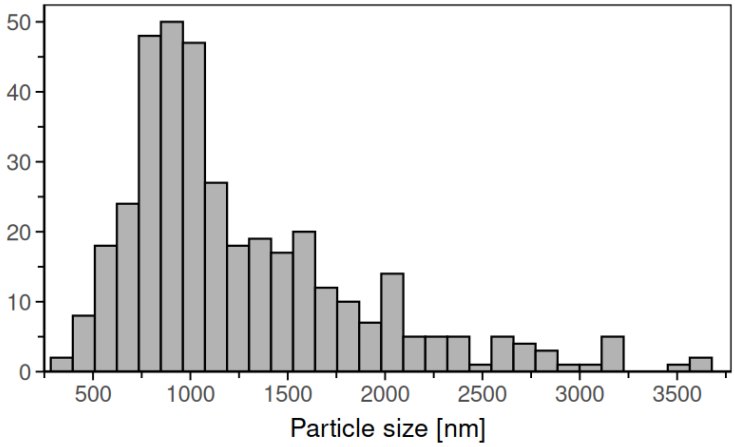

Fig. 5. Histogram of PHB/CHI size distribution obtained from SEM image analysis

Zeta potential analysis of the PHB/chitosan microspheres revealed a value of +52.36 ± 1.28 mV, indicating a strong positive surface charge due to chitosan protonation and, consequently, high colloidal stability of the dispersion. The monomodal zeta potential distribution further confirmed the chemical homogeneity of the particle surfaces. As shown in Fig. 6, the zeta potential decreased gradually with increasing pH, reflecting the deprotonation of amino groups on the chitosan surface. The isoelectric point was determined at approximately pH 8.26, above which the particles acquired a negative surface charge. This behavior confirms effective surface modification of PHB by the polymer.

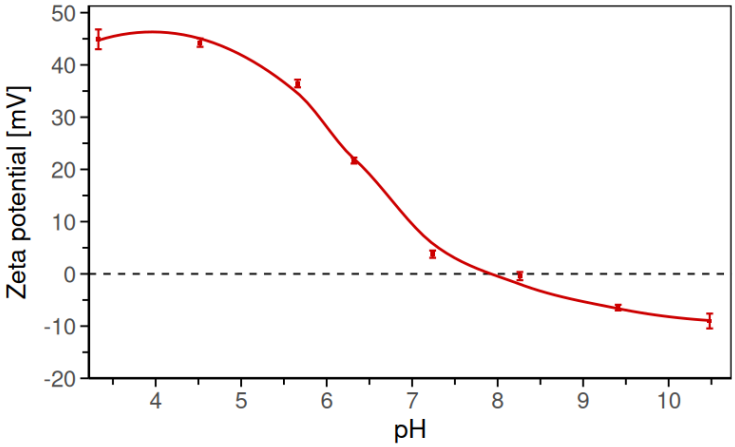

Fig 6. Zeta potential of PHB/CHI particles as a function of pH in a ionic strength of 10^{-3} M

3.2. Adsorption behavior of PHB/CHI microspheres on flat glass surfaces in clean water

In this study, the hydrophobic/hydrophilic properties of PHB/CHI microspheres were characterized by examining three-phase contact formation and by measuring advancing and receding contact angles, providing assessment of surface wettability.

For the clean glass surface, the advancing contact angle was below 4°, while the receding contact angle could not be measured, as a three-phase contact was not formed, leaving the bubble detached and separated from the solid surface by a thin liquid film. Deposition of positively charged PHB/CHI microspheres on the negatively charged glass surface significantly influenced surface hydrophobicity.

Even a 5-minute deposition under diffusion conditions from a 10 mg/L PHB/CHI solution increased the advancing contact angle to 39° . As shown in Fig. 7, 20 minutes of deposition resulted in the formation of a saturated layer with $\Theta_A \approx 50$, since further increases in deposition time had almost no effect on the contact angle. A similar effect was observed for the receding contact angle, with the exception that for samples with deposition times below 4 minutes, Θ_R could not be measured because a three-phase contact was not formed.

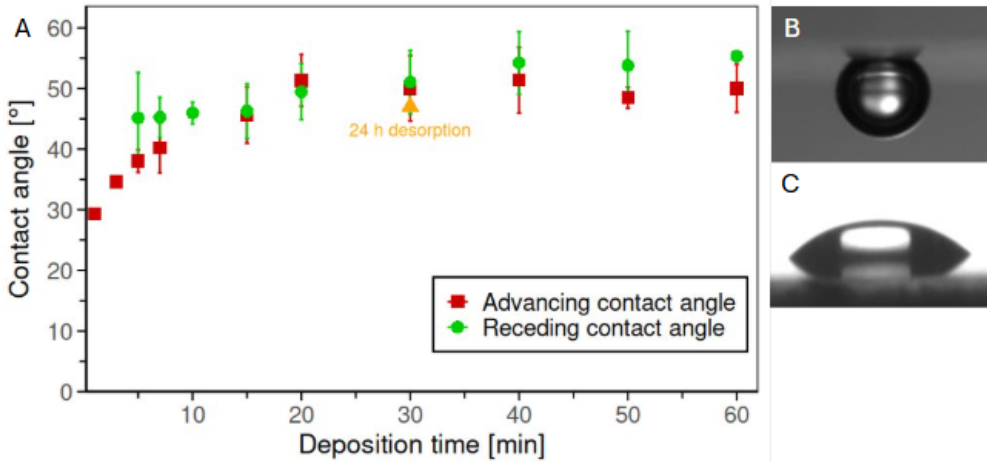

Fig. 7. (A) Contact angle of water on flat glass surfaces coated with PHB/CHI microspheres as a function of PHB/CHI microspheres deposition time. (B) Receding and (C) advancing contact angle images obtained for a surface coated for 30 min

To examine the stability of the PHB/CHI layer formed on the glass surface, samples with deposition times of 30 and 60 minutes were immersed in Milli-Q water for 24 hours. Remeasurement of the Θ_A revealed only a negligible decrease to 47°, indicating good stability of the deposited layer. The contact angle hysteresis (Θ_A - Θ_R) was below 10°, which indicates a smooth and chemically homogenous surface, suggesting uniform wetting behavior of the PHB/CHI coating.

The study of TPC formation on the modified glass surface revealed the existence of a threshold deposition time under the applied conditions, below which bubble-glass surface attachment did not occur. As shown in Fig. 8, starting from tdep = 5 min, the TPC was formed, with a sharp initial decrease in t_{TPC}, followed by a more gradual decline, reaching approximately 90 ms for tdep = 60 min. Since all measurements were performed in clean water, tbouncing had a constant value of 79 ± 4 ms. Therefore, the film drainage time followed the same trend as the TPC formation time, as described by Eq. (3). The decrease in $t_{drainage}$ with increasing deposition time indicates an enhancement of surface hydrophobicity, facilitating faster thinning and attachment.

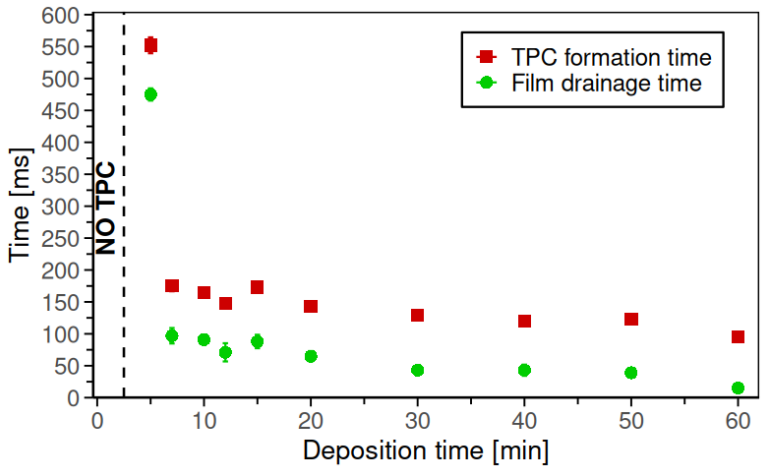

Fig. 8. Time of three-phase contact formation and time of film drainage in distilled water as a function of PHB/CHI microsphere deposition time on glass surfaces

Three dominant mechanisms can be identified for TPC formation (Niecikowska et al., 2012; Wiertel-Pochopien and Zawala, 2019): (i) changes in surface hydrophobicity, (ii) variations in surface roughness, and (iii) modification of surface charge. The interplay of these effects may be crucial for thin liquid film destabilization and subsequent TPC formation.

As PHB/chitosan microsphere deposition progresses, the surface becomes more hydrophobic, but only up to a certain degree. It was observed that, while the contact angle reached a plateau after 20 min of deposition time, the TPC formation time continued to decrease gradually with increasing deposition time. This phenomenon may result from two factors. First, even after the formation of a saturated layer, some free spots on the solid surface were likely still available and could be occupied by small PHB/CHI microspheres during prolonged deposition. This additional coverage did not significantly affect surface hydrophobicity and therefore had little impact on the contact angle. However, it could increase the surface charge, which strongly influenced interactions within the thin liquid film (Bueno-Tokunaga et al., 2015; Yang et al., 2001). The chitosan coating imparts a positive surface charge, which enhances electrostatic attraction to the negatively charged air bubble leading to film drainage. Second, possible variations in surface roughness induced by PHB/CHI microsphere adsorption may also contribute to TPC formation, as increased roughness facilitates local rupture and promotes three phase contact initiation. Moreover, this difference may have arisen from the distinct nature of the two measurements. The TPC formation time is a dynamic parameter, strongly dependent on the local surface properties at the point of contact, whereas contact angles describe an equilibrium state. This is also evident from the receding contact angle, which was measured after TPC formation: differences in t_{TPC} are not reflected in Θ_R.

It is important to note that control measurements were also performed for samples coated with chitosan only. Reference samples were prepared by immersing them in a 10 mg/L chitosan solution for 30 min. The advancing contact angle was only slightly higher than that of the clean glass surface, not exceeding 8°. In the case of TPC formation, the bubble did not attach to the surface even after several minutes. These results may indicate two scenarios: (i) very low surface coverage by chitosan macromolecules and/or (ii) the adsorbed chitosan maintains the surface in a hydrophilic state (Cohen and Poverenov, 2022; Zargar et al., 2015).

3.3. Adsorption behavior of PHB/CHI microspheres on flat glass surfaces in MIBC solution

Since froth flotation is carried out in the presence of a frother, it is important to evaluate the influence of its potential interactions with the PHB/CHI microspheres as collectors. Therefore, adsorption experiments were also conducted in the presence of MIBC, as a widely used as a frother.

Prior to measurement, the glass plate was thoroughly cleaned and subsequently immersed in a 10 mg/L PHB/CHI solution for 30 min to ensure the formation of a saturated PHB/CHI layer. A series of measurements of the contact angle (Fig. 9) and TPC formation time (Fig. 10) were then performed for various MIBC concentrations.

Fig. 9 presents the advancing (Θ_A) and receding (Θ_R) contact angle values measured on the prepared surfaces as a function of MIBC concentration. As observed, ΘA decreased by approximately 12° with increasing surfactant concentration, which can be explained by Young's equation (Blankschtein, 1989).

$$cos\theta = \frac{(\gamma_{SG} - \gamma_{SL})}{\gamma_{LG}} \tag{5}$$

Thus, knowing that $\gamma_{1x10^{-5}} = 72.0\ \frac{mN}{m}$, $\theta_{1x10^{-5}} = 49.7°$, and $\gamma_{6x10^{-3}} = 63.3\ \frac{mN}{m}$, the theoretical value of contact angle for $\theta_{6x10^{-3}}$ can be calculated as:

$$\theta_{6x10^{-3}} = \arccos\left(\frac{72.0\frac{mN}{m}\cdot\cos 49.7°}{63{,}3\frac{mN}{m}}\right) = 42{,}6° \tag{6}$$

The theoretical decrease in contact angle (≈7.1°) is in good agreement with the experimentally observed value (≈11.8°), indicating that the reduction in liquid–air surface tension is the dominant factor governing the wetting behavior.

Consequently, a decrease in surface tension at higher surfactant concentrations promotes enhanced spreading of the liquid over the solid surface. The slightly larger experimental decrease may suggest additional contributions from MIBC adsorption at the solid–liquid interface, further enhancing surface

wetting. The receding contact angle and hysteresis both increase with the concentration of MIBC. At very low concentrations the hysteresis remained below 10°, while above 6×10^{-5} M it already reached 14.95, and continued to rise with further increase in MIBC concentration. This trend indicates that the presence of MIBC modifies not only the air – liquid, but also the solid – liquid interfacial properties, affecting the mobility of the three – phase contact line.

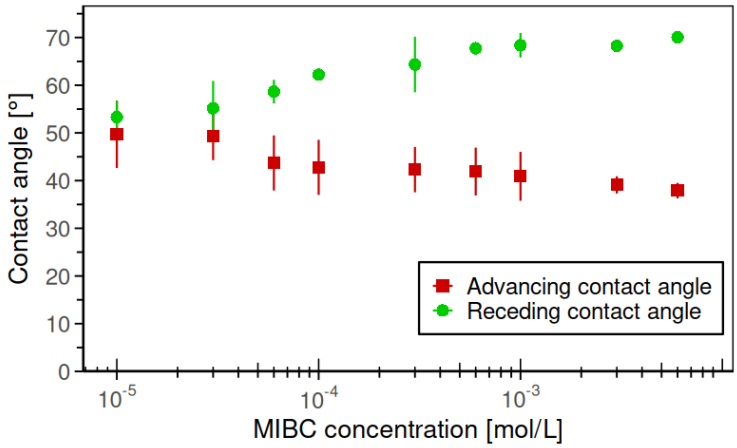

Fig. 9. Advancing and receding contact angles on the flat glass surfaces coated with PHB/CHI microspheres as a function of MIBC concentration

Fig. 10 shows the results for both the TPC formation time and the film drainage time. In the case of t_{TPC}, no clear trend with increasing MIBC concentration was observed, which can be attributed to the interplay of two competing effects. On one hand, the presence of MIBC in solution affected the bubble impact velocity through the formation of a dynamic adsorption layer over the rising bubble (Dukhin et al., 1995). As the surfactant concentration increased, the bubble velocity decreased, which led to a shorter bubble bouncing time (Malysa et al., 2005; Vakarelski et al., 2019). On the other hand, higher MIBC concentrations significantly prolonged the film drainage time. This effect is clearly visible in Fig. 10, where $t_{drainage}$ increased from ca. 80 ms at $c_{MIBC} = 1\times10^{-5}$ M to nearly 170 ms at $c_{MIBC} = 6\times10^{-3}$ M.

The prolongation of the film drainage time with concentration of MIBC can be explained by the adsorption of MIBC molecules at the air–water interface, which stabilizes the thin liquid film separating the bubble from the solid. As the surfactant concentration increases, the interfacial elasticity and surface viscosity rise, causing surface immobilization and reducing the rate of film thinning (Bournival et al., 2012; Wang and Yoon, 2006). This leads to slower drainage and, consequently, delays film rupture, counteracting the effect of reduced bubble velocity and shortening of $t_{bouncing}$. The observed balance between these two opposing mechanisms explains why t_{TPC} remains largely unaffected, while $t_{drainage}$ exhibits a strong dependence on the surfactant concentration.

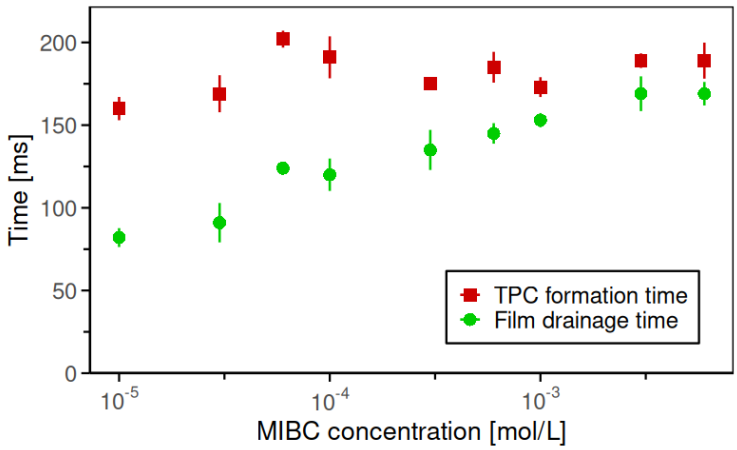

Fig. 10. Time of three-phase contact formation and time of film drainage as a function of MIBC concentration for the flat glass surfaces coated with PHB/CHI microspheres

From a flotation perspective, these results indicate that the presence of MIBC can influence bubble–particle attachment dynamics in the presence of PHB/CHI microspheres acting as collectors. Therefore, it is essential to optimize the frother dosage to minimize the negative effect associated with the increased stability of the thin liquid film, while the primary function of MIBC, i.e. the formation of a stable froth, is achieved.

3.4. Particle–bubble dynamic attachment

While contact angle and three-phase contact (TPC) formation measurements provide qualitative insights into the possible mechanisms of the designed flotation process, experiments that directly monitor the formation of particle–bubble aggregates are more informative in term of flotation processes.

According to the classical flotation model (Wang et al., 2016), the overall probability of bubble–particle aggregate formation (P) can be expressed as the product of three subprocesses: collision (Pc), attachment (Pa) and detachment (Pd) probabilities. While TPC measurements reflect only the attachment probability (assuming Pc = 1 and Pd = 0), direct visualization of particle-bubble attachment provides a quantitative link between interfacial phenomena and the macroscopic flotation response.

Therefore, using our custom-made apparatus, three series of experiments were carried out (Fig. 11). In the first series, quartz was tested in PHB/CHI microsphere solutions of varying concentrations to evaluate the effect of collector dosage. In the second series, the same conditions were applied, but with the addition of MIBC at 1.6×10^{-2} M, to assess the combined influence of microspheres as collectors and the frother, and maintain the same conditions as in the tested flotation process. Third series was control measurement, in which quartz was examined in a chitosan solution alone to distinguish the specific role of the microsphere coating.

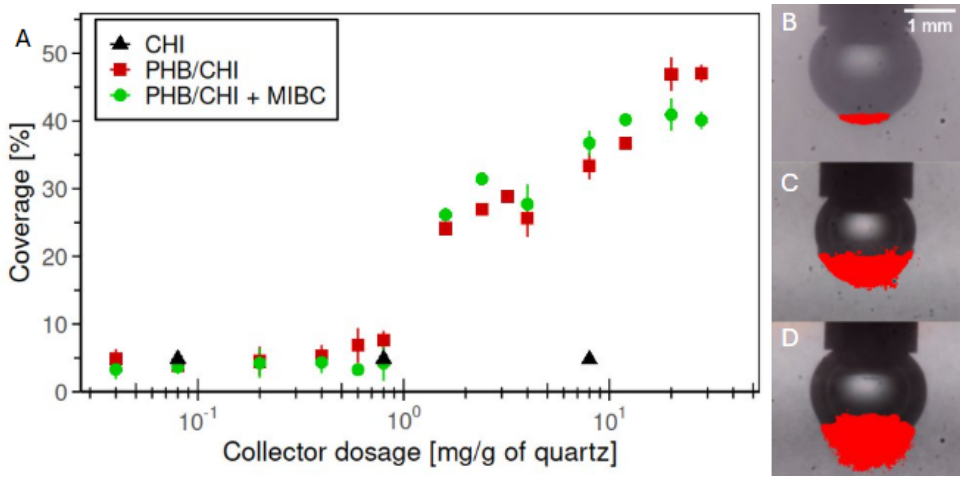

Fig. 11. (A) Coverage data for three series of measurements of quartz suspended in: (▲) chitosan solution, (■) PHB/CHI microsphere solution, and (●) PHB/CHI microsphere solution with the addition of MIBC at 1.6×10^{-2} M. (B-D) Representative post-processed images illustrating bubble-grain aggregates formed in: (B) CHI, (C) PHB/CHI and (D) PHB/CHI + MIBC. All images were obtained for a collector dosage of 0.8 mg per 1 g of quartz

Fig. 11 shows that PHB/CHI microspheres significantly increased quartz coverage over the bubble surface, with a sharp rise for c_{PHB}/CHI > 1.6 mg/ g of quartz, reaching ca. 25–30% bubble coverage at the highest tested concentrations.

These results are in very good agreement with the contact angle and TPC formation measurements. All three experimental methods consistently highlight the crucial role of the collector in the quartz recovery. In both, contact angle and TPC formation experiments, greater surface coverage by PHB/CHI microspheres led to enhanced hydrophobization of the solid surface. Likewise, increasing the PHB/CHI microsphere concentration in the particle-bubble attachment experiment resulted in a higher load of quartz particles on the bubble surface.

It is interesting that, although the TPC formation measurements clearly demonstrate that MIBC stabilizes the thin liquid film and prolongs the drainage time, the particle–bubble dynamic attachment

results suggest that MIBC does not noticeably affect the efficiency of particle attachment. This indicates that TPC studies primarily capture kinetic effects and the timescale of film thinning, rather than providing information about interfacial coverage or the extent of particle adsorption, which is better reflected by the dynamic attachment measurements. The observed lack of a statistically significant change in bubble – particle attachment and quartz recovery, suggests that MIBC did not noticeably affect how efficiency the particles attached.

In contrast, chitosan alone exhibited very low surface coverage across the entire concentration range, not exceeding ~7%. This confirms that the presence of PHB/CHI microspheres was essential to achieving significant hydrophobization of quartz surfaces. In quartz flotation, chitosan adsorbs onto the negatively charged silica surface via hydrogen bonding and electrostatic attraction, forming a hydrophilic layer that prevent collector adsorption and bubble attachment. This mechanism result in selective depression of quartz in mixed mineral systems (Tiraferri et al., 2014).

3.5. Quartz flotation

The froth flotation tests of quartz particles (50–100 μm) were conducted at a constant MIBC concentration. The effect of the PHB/CHI microspheres dosage on quartz recovery as a function of flotation time was evaluated. Additionally, the experiments performed in the presence of MIBC only and chitosan with MIBC served as references.

Fig. 12 present quartz recovery as a function of time under different collector conditions. In the collectorless flotation (0.0 mg/g of quartz), recovery increased slowly and remained modest throughout the test, reaching only ca. 45–55 % at 60 min. The recovered fraction likely resulted from the mechanical entrainment and occasional transient bubble–grain contacts. This effect is consistent with the presence of a fine particle fraction (<50 μm), which is known to enhance recovery through entrainment rather than true flotation.

When chitosan was used alone (0.08 mg/g of quartz) with MIBC, recoveries were similarly low. This confirms that chitosan, despite its cationic nature, does not promote quartz hydrophobicity and may even act as a depressant under these conditions, which is consistent with the trends observed in the TPC and contact angle measurements. The flotation rate was calculated from the formula (Polat and Chander, 2000):

$$R(t) = R_{\infty}\left(1 - \int_0^{\infty} f(k)\exp(-kt)\,dk\right) \tag{6}$$

The addition of PHB/CHI microspheres significantly enhanced both the initial flotation rate and the quartz recovery, with a clear dosage-dependent effect. At the collector concentration of 0.008 mg/g of quartz, the recovery steadily increased to ca. 65 % after 60 min and flotation rate was equal 0.0397 s-1. Increasing the dosage to 0.08 mg/g of quartz further accelerated the kinetics to 0.0515 s^{-1} and improved the recovery to ca. 80 %. At the highest tested dosages, 0.8 mg/g of quartz, the recovery increased to 90%, indicating faster kinetic 0.0587 s-1 and more stable bubble–particle attachment.

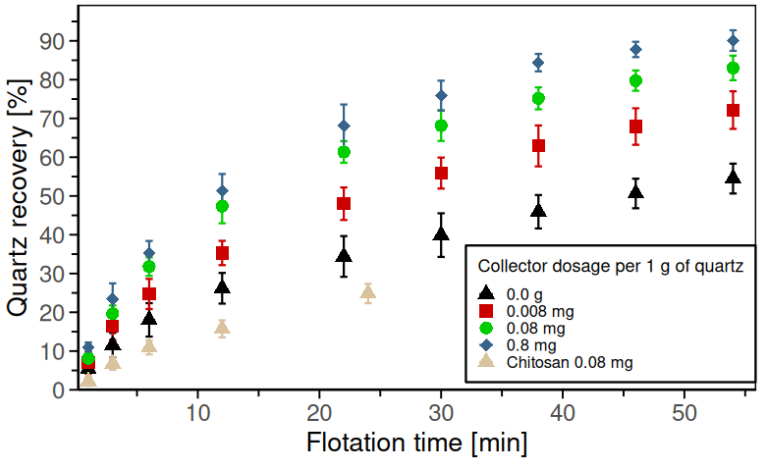

Fig. 12. Quartz recovery as a function of flotation time for different collectors' concentration. Process conditions: c_{MIBC} = 1.6×10-2 M, tconditioning = 4 min

In addition to dosage test, the effect of conditioning time was examined at fixed collector concentrations of 0.08 mg/g of quartz, which was selected as it provided a substantial improvement in recovery while maintaining reasonable reagent consumption. This test aimed to assess the adsorption efficiency and kinetics of the PHB/CHI microspheres.

The results presented in Fig. 13 demonstrate that the flotation performance of quartz with PHB/CHI microspheres was essentially unaffected by conditioning time. The adsorption and activation of the PHB/CHI microspheres on the quartz surface occur rapidly and reach equilibrium within the first minute of conditioning. This finding suggests that the microsphere deposition process is highly efficient and does not require prolonged agitation prior flotation. Consequently, short conditioning times can be applied without compromising recovery, highlighting the practical potential of PHB/CHI microspheres as fast-acting, biodegradable collectors.

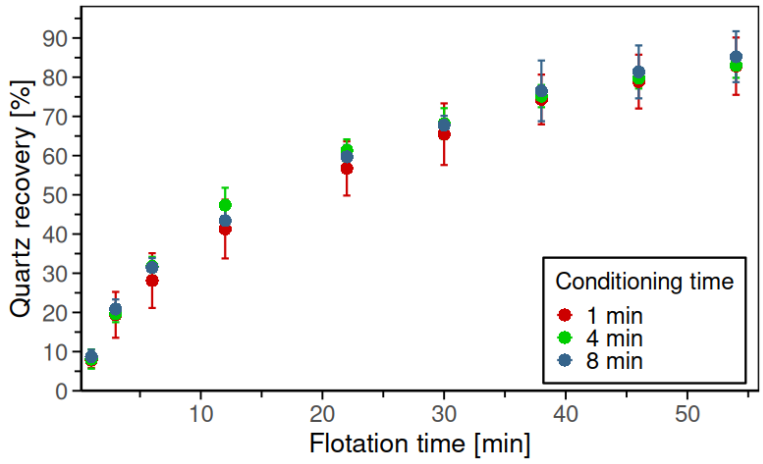

Fig. 13. Quartz recovery as a function of flotation time for different conditioning times. PHB/CHI microspheres concentration: 0.08 mg per 1 g of quartz. Process conditions: c_{MIBC} = 1.6×10^{-2} M

6. Conclusions

This study demonstrated that PHB/CHI microspheres act as efficient bio-based collectors, biodegradable collectors capable of substantially enhancing quartz flotation. The observed high polydispersity of PHB/CHI microspheres may be advantageous as their adsorption increases the probable surface roughness which improve the flotation efficiency (Cheng et al., 2024; Krasowska and Malysa, 2007; Zhao et al., 2023). Moreover, larger microspheres may act as binders for fine particles, facilitating their aggregation into larger, more easily floatable clusters, and thereby enhancing particle-bubble attachment (Farrokhpay et al., 2021; Huang et al., 2020).

Flotation tests revealed a clear dosage-dependent improvement in both flotation kinetics and recovery, with PHB/CHI concentrations as low as 0.08 mg per 1 g of quartz providing a notable effect (recovery ca. 80%). The paper showed that microsphere adsorption increased the contact angles and accelerated three-phase contact formation, indicating effective hydrophobization of quartz surfaces.

Particle-bubble attachment experiments supported this mechanism, showing markedly higher bubble coverage with quartz particles in the presence of PHB/CHI microspheres, whereas chitosan alone produced negligible attachment, consistent with its hydrophilic and depressant character. The addition of MIBC did not statistically influence the coverage of bubble with quartz particles. This limited synergy was in line with TPC results, which demonstrated that MIBC stabilizes the wetting film and prolongs drainage. These findings highlight the importance of optimizing the of frother dosage when combining MIBC with biopolymer-based collectors.

It should be emphasized that although chitosan is widely known as a hydrophilic depressant for many silicate minerals, its role in the PHB/CHI composite is fundamentally different. Chitosan alone does not increase quartz hydrophobicity, consistent with its depressant behavior. In the PHB/CHI microspheres, however, chitosan acts primarily as a cationic anchoring component that promotes attachment of the composite particle to the negatively charged quartz surface. The hydrophobicity

responsible for flotation enhancement arises from the exposed PHB domains rather than from chitosan itself. This distinction explains why chitosan alone remains hydrophilic but contributes functionally to the collector system when incorporated into the composite structure.

Overall, the results establish PHB/CHI microspheres as a promising bio-based alternative to conventional amine-based flotation reagents. Further work should focus on selectivity tests with multi-mineral systems, and evaluation of collector biodegradability under process conditions.

Acknowledgement

This research was financially supported by the Polish National Science Centre (NCN, grant no. 2020/38/E/ST8/00173) and by the Polish National Agency for Academic Exchange (NAWA) under the Programme STER- Internationalisation of doctoral schools (project no. BPI/STE/2023/1/00027/U/00001). The authors wish to thank Dr. Dorota Duraczyńska for her kind assistance and for carrying out the SEM measurements essential to this study. The authors gratefully acknowledge the Mineral Processing Laboratory at the Norwegian University of Science and Technology (NTNU) for providing access to experimental facilities and technical support. Special thanks are extended to Mr. Kornel Tobiczyk from NTNU for his valuable assistance during the laboratory work. I wish to acknowledgment the contribution of Mr. Łukasz Witkowski from the ICSC, Polish Academy of Sciences in Cracow, for his invaluable technical assistance.

References

ABARCA, C., ALI, M.M., PELTON, R.H., 2018. *Choosing mineral flotation collectors from large nanoparticle libraries.* J. Colloid Interface Sci. 516, 423–430.

ABARCA, C., YANG, S., PELTON, R.H., 2015. *Towards high throughput screening of nanoparticle flotation collectors.* J. Colloid Interface Sci. 460, 97–104.

ALSAFASFEH, A., ALAGHA, L., O'KEEFE, T.J., 2023. *Chitosan as an Eco-Friendly Alternative for Silicate Depressant in Phosphate Flotation,* Journal of Engineering and Chemical Industries, 6(2), 34-38.

ALTAEE, N., EL-HITI, G.A., FAHDIL, A., SUDESH, K., YOUSIF, E., 2016. *Biodegradation of different formulations of polyhydroxybutyrate films in soil*. Springerplus 5.

ARAUJO, A.C., VIANA, P.R.M., PERES, A.E.C., 2005. *Reagents in iron ores flotation.* Miner. Eng. 18, 219–224.

ASIMI NEISIANI, A., SANEIE, R., MOHAMMADZADEH, A., WONYEN, D.G., CHEHREH CHELGANI, S., 2023. *Polysaccharides-based pyrite depressants for green flotation separation: An overview.* Int. J. Min. Sci. Technol. 33, 1229–1241.

BEDNAREK, P.S., ZAWALA, J., KOWALCZUK, P.B., 2025. *Polymer-based collectors in flotation: A review.* Adv. Colloid Interface Sci., 335, 103351.

BEHERA, S.K., MULABA-BAFUBIANDI, A.F., 2017. *Microbes Assisted Mineral Flotation a Future Prospective for Mineral Processing Industries: A Review.* Mineral Processing and Extractive Metallurgy Review, 38, 96-105.

BLANKSCHTEIN, D., 1989. *Colloidal systems and interfaces by S.* Ross and I. D. Morrison, Wiley-Interscience, New York, 1988, 422, pp.,. AIChE Journal 35.

BOURNIVAL, G., PUGH, R.J., ATA, S., 2012. *Examination of NaCl and MIBC as bubble coalescence inhibitor in relation to froth flotation*. Miner. Eng. 25, 47–53.

BUDEMBERG, G., JOLSTERÅ, R., CHELGANI, S.C., 2025. *Eco-friendly collectors in apatite froth flotation: A review*. Int. J. Min. Sci. Technol. 35, 539–551.

BUENO-TOKUNAGA, A., PÉREZ-GARIBAY, R., MARTÍNEZ-CARRILLO, D., 2015. *Zeta potential of air bubbles conditioned with typical froth flotation reagents.* Int. J. Miner. Process. 140.

CHENG, G., XIONG, L., LU, Y., ZHANG, Z.G., LV, C., LAU, E. V., 2024. *Advancements in the application of surface roughness in mineral flotation process.* Separation Science and Technology (Philadelphia).

CHIELLINI, E., CORTI, A., D'ANTONE, S., SOLARO, R., 2003. *Biodegradation of poly (vinyl alcohol) based materials.* Prog Polym Sci 28, 963–1014.

COHEN, E., POVERENOV, E., 2022. *Hydrophilic Chitosan Derivatives: Synthesis and Applications.* Chemistry - A European Journal, 28, e202202156.

DHAR, P., HAVSKJOLD, H., THORNHILL, M., ROELANTS, S., SOETAERT, W., KOTA, H.R., CHERNYSHOVA, I., 2021. *Toward green flotation: Interaction of a sophorolipid biosurfactant with a copper sulfide.* J. Colloid Interface Sci. 585, 386–399.

DUKHIN, S.S., KRETZSCHMAR, G., MILLER, R., 1995. *Dynamics of Adsorption at Liquid Interfaces - Theory, Experiment, Application.* Elsevier Science B. V. 1.

FARROKHPAY, S., FILIPPOV, L., FORNASIERO, D., 2021. *Flotation of Fine Particles: A Review.* Mineral Processing and Extractive Metallurgy Review.

FARUGA, A., CICHOŃ, E., KARCZ, R., KRYŚCIAK-CZERWENKA, J., SZUMERA, M., PRAJSNAR, J., GUZIK, M., 2025. *Integrated chemo-biotechnological process for upcycling polyesters into new PHB.* Biotechnology for the Environment 2, 11.

FRANCIS, L., MENG, D., KNOWLES, J., KESHAVARZ, T., BOCCACCINI, A.R., ROY, I., 2011. *Controlled delivery of gentamicin using poly(3-hydroxybutyrate) microspheres.* Int J Mol Sci 12, 4294–4314.

FRANCIS, L., MENG, D., KNOWLES, J.C., ROY, I., BOCCACCINI, A.R., 2010. *Multi-functional P(3HB) microsphere/45S5 Bioglass®-based composite scaffolds for bone tissue engineering.* Acta Biomater 6, 2773–2786.

GANAPATHY, K., RAMASAMY, R., DHINAKARASAMY, I., 2018. *Polyhydroxybutyrate production from marine source and its application.* Int J Biol Macromol 111, 102–108.

GOVENDER, Y., GERICKE, M., 2011. *Extracellular polymeric substances (EPS) from bioleaching systems and its application in bioflotation,* Min. Eng. 24(11), 1122-1127..

GUNGOREN, C., OZDEMIR, O., OZKAN, S.G., 2025. *Surface Properties and Beneficiation of Quartz with Flotation.* Minerals..

HAJATI, A., SHAFAEI, S.Z., NOAPARAST, M., FARROKHPAY, S., ASLANI, S., 2016. *Novel application of talc nanoparticles as collector in flotation.* RSC Adv 6, 98096–98103.

HAN, Y., GUO, W., ZHU, Y., WEI, Y., GU, X., 2018. *Flotation behavior and separation mechanism of quartz and iron minerals in a-bromolauric acid reverse flotation system.* Physicochem. Probl. Miner. Process. 54.

HAYAT, M.B., ALAGHA, L., SANNAN, S.M., 2017. *Flotation Behavior of Complex Sulfide Ores in the Presence of Biodegradable Polymeric Depressants.* Int J Polym Sci 2017.

HERRERA URBINA, R., 2003. *Recent developments and advances in formulations and applications of chemical reagents used in froth flotation.* Mineral Processing and Extractive Metallurgy Review.

HUANG, G., XU, J., GENG, P., LI, J., 2020. *Carrier flotation of low-rank coal with polystyrene.* Minerals. 10.

IBRAHIM, M.H.A., STEINBÜCHEL, A., 2009. *Poly(3-hydroxybutyrate) production from glycerol by Zobellella denitrificans MW1 via high-cell-density fed-batch fermentation and simplified solvent extraction.* Appl Environ Microbiol 75, 6222–6231.

JIANG, H., ZHANG, Y., BIAN, K., WANG, C., XIE, X., WANG, H., ZHAO, H., 2022. *Is it possible to efficiently and sustainably remove microplastics from sediments using froth flotation? Chemical Engineering Journal 448, 137692.*

KORDLOO, M., KHODADADMAHMOUDI, G., EBRAHIMI, E., REZAEI, A., TOHRY, A., CHEHREH CHELGANI, S., 2023. *Green hematite depression for reverse selective flotation separation from quartz by locust bean gum.* Sci. Rep. 13.

KOSIOR, D., ZAWALA, J., MALYSA, K., 2014. *Influence of n-octanol on the bubble impact velocity, bouncing and the three phase contact formation at hydrophobic solid surfaces.* Colloids Surf. A Physicochem. Eng. Asp. 441, 788–795.

KRASOWSKA, M., MALYSA, K., 2007. *Kinetics of bubble collision and attachment to hydrophobic solids: I.* Effect of surface roughness. Int. J. Miner. Process. 81, 205–216.

LARSEN, E., KOWALCZUK, P.B., KLEIV, R.A., 2019. *Non-HF collectorless flotation of quartz.* Miner. Eng. 133, 115–118.

LASKOWSKI, J.S., 2010. *A new approach to classification of flotation collectors, in: Canadian Metallurgical Quarterly.*

LECETA, I., GUERRERO, P., CABEZUDO, S., DE LA CABA, K., 2013. *Environmental assessment of chitosan-based films.* J Clean Prod 41, 312–318.

LIMA, N.P., VALADÃO, G.E.S., PERES, A.E.C., 2013. *Effect of amine and starch dosages on the reverse cationic flotation of an iron ore.* Miner. Eng. 45, 180–184.

MALYSA, K., KRASOWSKA, M., KRZAN, M., 2005. *Influence of surface active substances on bubble motion and collision with various interfaces.* Adv. Colloid Interface Sci, 114-115, 205-225.

MARUŠINCOVÁ, H., HUSÁROVÁ, L., RŮŽIČKA, J., INGR, M., NAVRÁTIL, V., BUŇKOVÁ, L., KOUTNY, M., 2013. *Polyvinyl alcohol biodegradation under denitrifying conditions.* Int Biodeterior Biodegradation 84, 21–28.

MCADAM, B., FOURNET, M.B., MCDONALD, P., MOJICEVIC, M., 2020. *Production of polyhydroxybutyrate (PHB) and factors impacting its chemical and mechanical characteristics.* Polymers (Basel), 12(12).

MELO, F., LASKOWSKI, J.S., 2006. *Fundamental properties of flotation frothers and their effect on flotation.* Miner. Eng. 19.

NAGARAJ, D.R., FARINATO, R.S., 2016. *Evolution of flotation chemistry and chemicals: A century of innovations and the lingering challenges.* Miner. Eng. 96–97, 2–14.

NASIRIMOGHADDAM, S., MOHEBBI, A., KARIMI, M., REZA YARAHMADI, M., 2020. *Assessment of pH-responsive nanoparticles performance on laboratory column flotation cell applying a real ore feed.* Int. J. Min. Sci. Technol. 30, 197–205.

NIECIKOWSKA, A., KRASOWSKA, M., RALSTON, J., MALYSA, K., 2012. *Role of surface charge and hydrophobicity in the three-phase contact formation and wetting film stability under dynamic conditions.* Journal of Physical Chemistry C., 116(4).

OLALLA, A.L., SARA, L.I., RICARDO, B., 2021. *Assessment of toxicity and biodegradability of poly(Vinyl alcohol)-based materials in marine water.* Polymers (Basel) 13.

PELEKA, E.N., GALLIOS, G.P., MATIS, K.A., 2018. *A perspective on flotation: a review.* Journal of Chemical Technology and Biotechnology.

PETER, M.G., 1995. *Applications and Environmental Aspects of Chitin and Chitosan.* Journal of Macromolecular Science, Part A 32, 629–640.

POLAT, M., CHANDER, S., 2000. *First-order flotation kinetics models and methods for estimation of the true distribution of flotation rate constants.* Int. J. Miner. Process. 58, 145–166.

RAJAN, K.P., THOMAS, S.P., GOPANNA, A., CHAVALI, M., 2019. *Polyhydroxybutyrate (PHB): A standout biopolymer for environmental sustainability,* in: Handbook of Ecomaterials., L.M. Torres Martínez, O.V. Kharissova, B.I. Kharisov eds., Springer Cham.

RAMOS-ESCOBEDO, G.T., PECINA-TREVIÑO, E.T., BUENO TOKUNAGA, A., CONCHA-GUERRERO, S.I., RAMOS-LICO, D., GUERRA-BALDERRAMA, R., ORRANTIA-BORUNDA, E., 2016. *Bio-collector alternative for the recovery of organic matter in flotation processes.* Fuel 176, 165–172.

REHM, B.H.A., 2010. *Bacterial polymers: Biosynthesis, modifications and applications.* Nat Rev Microbiol., 8, pages 578–592.

RUBIO, J., SOUZA, M.L., SMITH, R.W., 2002. *Overview of flotation as a wastewater treatment technique.* Miner. Eng. 15.

SAWAGUCHI, A., ONO, S., OOMURA, M., INAMI, K., KUMETA, Y., HONDA, K., SAMESHIMA-SAITO, R., SAKAMOTO, K., ANDO, A., SAITO, A., 2015. *Chitosan degradation and associated changes in bacterial community structures in two contrasting soils.* Soil Sci Plant Nutr 61, 471–480.

SIGAUKE, T., JOHNSON, O.T., NDESHIMONA, V.L., MASHINGAIDZE, M.M., 2025. *Advancements in nanotechnology for the enhanced flotation of fine mineral particles: a review.* Discover Applied Sciences.

TIRAFERRI, A., MARONI, P., CARO RODRÍGUEZ, D., BORKOVEC, M., 2014. *Mechanism of chitosan adsorption on silica from aqueous solutions.* Langmuir 30, 4980–4988.

TOHRY, A., DEHGHAN, R., DE SALLES LEAL FILHO, L., CHEHREH CHELGANI, S., 2021. *Tannin: An eco-friendly depressant for the green flotation separation of hematite from quartz.* Miner. Eng. 168.

VAKARELSKI, I.U., YANG, F., TIAN, Y.S., LI, E.Q., CHAN, D.Y.C., THORODDSEN, S.T., 2019. *Mobile-surface bubbles and droplets coalesce faster but bounce stronger.* Sci Adv 5(10).

WANG, G., NGUYEN, A. V., MITRA, S., JOSHI, J.B., JAMESON, G.J., EVANS, G.M., 2016. *A review of the mechanisms and models of bubble-particle detachment in froth flotation.* Sep. Purif. Technol., 170, 155-172.

WANG, L., YOON, R.H., 2006. *Role of hydrophobic force in the thinning of foam films containing a nonionic surfactant.* Colloids Surf. A Physicochem. Eng. Asp. 282–283, 84–91.

WEI, D.X., DAO, J.W., LIU, H.W., CHEN, G.Q., 2018. *Suspended polyhydroxyalkanoate microspheres as 3D carriers for mammalian cell growth.* Artif Cells Nanomed Biotechnol 46, 473–483.

WIERTEL-POCHOPIEN, A., KOSIOR, D., ZAWALA, J., 2021. *Effect of dynamic adsorption layer over colliding bubble on rate of solid surface dewetting in cationic surfactant solutions.* Miner. Eng. 165.

WIERTEL-POCHOPIEN, A., ZAWALA, J., 2019. *Rupture of Wetting Films Formed by Bubbles at a Quartz Surface in Cationic Surfactant Solutions.* Chem. Eng. Technol. 42.

YANG, C., DABROS, T., LI, D., CZARNECKI, J., MASLIYAH, J.H., 2001. *Measurement of the zeta potential of gas bubbles in aqueous solutions by microelectrophoresis method.* J. Colloid Interface Sci. 243.

YANG, H.F., LI, T., CHANG, Y.H., LUO, H., TANG, Q.Y., 2014. *Possibility of using strain F9 (Serratia marcescens) as a bio-collector for hematite flotation.* International Journal of Minerals., Metallurgy and Materials 21, 210–215.

YANG, S., PELTON, R., RAEGEN, A., MONTGOMERY, M., DALNOKI-VERESS, K., 2011. *Nanoparticle flotation collectors: Mechanisms behind a new technology.* Langmuir 27, 10438–10446.

YE, B., LI, Y., CHEN, Z., WU, Q.Y., WANG, W.L., WANG, T., HU, H.Y., 2017. *Degradation of polyvinyl alcohol (PVA) by UV/chlorine oxidation: Radical roles, influencing factors, and degradation pathway.* Water Res 124, 381–387.

ZALLOUM, N.L., ALBINO DE SOUZA, G., MARTINS, T.D., 2019. *Single-Emulsion P(HB-HV) Microsphere Preparation Tuned by Copolymer Molar Mass and Additive Interaction.* ACS Omega 4, 8122–8135.

ZARGAR, V., ASGHARI, M., DASHTI, A., 2015. *A Review on Chitin and Chitosan Polymers: Structure, Chemistry, Solubility, Derivatives, and Applications.* ChemBioEng Reviews, 2, 204-226.

ZAWALA, J., KARAGUZEL, C., WIERTEL, A., SAHBAZ, O., MALYSA, K., 2017. *Kinetics of the bubble attachment and quartz flotation in mixed solutions of cationic and non-ionic surface-active substances.* Colloids Surf. A Physicochem. Eng. Asp. 523, 118–126.

ZAWALA, J., NIECIKOWSKA, A., 2017. *"Bubble-on-demand "generator with precise adsorption time control.* Review of Scientific Instruments 88.

ZHANG, M., THOMAS, N.L., 2011. *Blending polylactic acid with polyhydroxybutyrate: The effect on thermal, mechanical, and biodegradation properties.* Advances in Polymer Technology 30, 67–79.

ZHANG, W., SUN, W., HU, Y., CAO, J., GAO, Z., 2019. *Selective flotation of pyrite from Galena using Chitosan with different molecular weights.* Minerals. 9.

ZHAO, L., ZHOU, J., ZHANG, Z. JUN, LIU, Q. XIA, 2023. *Fundamental role of surface roughness in bubble-particle interaction in flotation: A review.* J Cent South Univ., 30(9), 3021-3043.